Electron correlations in the effective-potential expansion method

Yasutami Takada
Institute for Solid State Physics, University of Tokyo, Roppongi, Minato-ku, Tokyo 106, Japan
(Received 17 July 1986)

The method of effective-potential expansion is successfully applied to a three-dimensional electron gas. Calculated correlation energies agree quite well with accurate Monte Carlo data. The difference is less than 1% for $1 \leqq r_s \leqq 10$. The static structure factor and pair-distribution function are also calculated. The latter is found to be always positive for these densities.

I. INTRODUCTION

The method of effective-potential expansion for the many-body problem was formulated by the present author a few years ago[1] and applied to a two-dimensional electron gas in a previous paper,[2] hereafter referred to as I. Since we have already explained motivations for the introduction of the method in I, we will not repeat them here. We have only to mention that the essential idea of the method is the introduction of an effective potential $\tilde{V}$, in terms of which any physical quantity is expanded. A variational procedure is used to determine $\tilde{V}$.

In I, we employed an approximation in which all terms higher than second order in $\tilde{V}$ were neglected. (We denoted as the two-body approximation the cutoff of our cluster expansion at this level.) In addition, when we determined $\tilde{V}$ variationally, we first assumed some functional form (such as a Thomas-Fermi–type screened potential) for $\tilde{V}$ and then chose optimum values for parameters involved in the function. Even in such a crude approximation, we obtained the results for the correlation energy ε_c in a two-dimensional electron gas in rather good agreement with those given by the variational Monte Carlo method.[3] (The difference was within several percent for $1 < r_s < 100$.) However, the major problem was that the spin-antiparallel pair-distribution function $g_{\uparrow\downarrow}(r)$ became negative near $r=0$ for $r_s \geqq 2.5$.

In the present paper, we apply the method to a three-dimensional electron gas. Compared to the numerical procedure in I, we have developed the method in two aspects: One is that we have determined $\tilde{V}$ by a numerical solution of an Euler-Lagrange–type equation. The other is that we have gone beyond the two-body approximation. Namely, besides all terms up to second order in $\tilde{V}$, we have included the ring terms in third and fourth orders in $\tilde{V}$, together with their exchange partners so as to make the Pauli principle hold order by order. As a result of these improvements, we have obtained ε_c in quite good agreement with the essentially exact Monte Carlo data of Ceperley and Alder.[4] (The difference is less than 1% for $1 \leqq r_s \leqq 10$.) We have also found that $g_{\uparrow\downarrow}(r)$ is always positive.

In Sec. II, we give a brief account of the method and show calculated results in the two-body approximation. Some of the higher-order terms are included in Sec. III. Results for ε_c, $g_{\uparrow\downarrow}(r)$, and the spin-dependent static structure factor $S_{\sigma\sigma'}(q)$ are compared with those obtained by several other methods. In Sec. IV, we summarize our results and discuss spin dependence of $\tilde{V}$. In the Appendix, we prove rigorously that the energy evaluated in the two-body approximation gives an upper bound to the ground-state energy for sufficiently weak effective potentials.

II. TWO-BODY APPROXIMATION

A. Preliminaries

Since the formalism is just the same as that in I, we give only a brief description of it here. The Hamiltonian of an electron gas in a uniform positive background is written as

$$H = H_0 + V \ , \tag{1}$$

where

$$H_0 = \sum_{\mathbf{k},\sigma} \varepsilon_{\mathbf{k}} C^{\dagger}_{\mathbf{k}\sigma} C_{\mathbf{k}\sigma} \ , \tag{2}$$

and

$$V = \tfrac{1}{2} \sum_{\mathbf{q}\,(\neq 0)} \sum_{\mathbf{k},\sigma} \sum_{\mathbf{k}',\sigma'} V(q) C^{\dagger}_{\mathbf{k}+\mathbf{q}\sigma} C^{\dagger}_{\mathbf{k}'-\mathbf{q}\sigma'} C_{\mathbf{k}'\sigma'} C_{\mathbf{k}\sigma} \ , \tag{3}$$

with $\varepsilon_{\mathbf{k}} = \hbar^2\mathbf{k}^2/2m$ and $V(q) = 4\pi e^2/q^2$. As usual, $C_{\mathbf{k}\sigma}$ is the destruction operator of an electron specified by wave vector $\mathbf{k}$ and spin σ. In the following, we measure momenta and energies in units of the Fermi momentum $\hbar k_F$ and rydbergs $me^4/2\hbar^2$, respectively. Then the system can be described by only one parameter r_s, defined by $r_s = me^2/\alpha\hbar^2 k_F$ with $\alpha \equiv (4/9\pi)^{1/3} = 0.521$.

For the ground-state wave function, we consider the following trial function:

$$|\Phi_0\rangle = \sum_{n=0}^{\infty} \frac{1}{n!} \left[-\frac{i}{\hbar} \right]^n \times L_u \left[\int_{-\infty}^{0} dt\, e^{0^+ t} e^{iH_0 t/\hbar} \tilde{V} e^{-iH_0 t/\hbar} \right]^n |0\rangle \ , \tag{4}$$

where $|0\rangle$ is the state described by a plane-wave Slater determinant, and $\tilde{V}$ is an effective potential, defined by

$$\tilde{V} = \tfrac{1}{2} \sum_{\mathbf{q}(\neq 0)} \sum_{\mathbf{k},\sigma} \sum_{\mathbf{k}',\sigma'} \tilde{V}_{\sigma\sigma'}(q) C^{\dagger}_{\mathbf{k}+\mathbf{q}\sigma} C^{\dagger}_{\mathbf{k}'-\mathbf{q}\sigma'} C_{\mathbf{k}'\sigma'} C_{\mathbf{k}\sigma} \ . \tag{5}$$

The symbol L_u in Eq. (4) represents the instruction to consider only terms in which each $\tilde{V}$ in $\tilde{V}^n$ is unlinked to others. The effective potential $\tilde{V}_{\sigma\sigma'}(q)$ in Eq. (5) will be determined variationally, but in Secs. II and III, we will neglect the spin dependence of $\tilde{V}$. Therefore we will suppress the subscript $\sigma\sigma'$ for the time being. (We will discuss dependence of $\tilde{V}$ on spin orientations in Sec. IV.)

The expectation value of the Hamiltonian with respect to the trial function (4) is given by the following cluster expansion:

$$\langle H\rangle=\langle\Phi_0\,|\,H\,|\,\Phi_0\rangle/\langle\Phi_0\,|\,\Phi_0\rangle=\sum_{n=0}^{\infty}E^{(n)}\ , \tag{6}$$

where $E^{(0)}$ is the Hartree-Fock energy, given by

$$E^{(0)}=N(2.21/r_s^2-0.916/r_s)\ , \tag{7}$$

with N being the total number of electrons, and for $n\geqq 1$,

$$E^{(n)}=C_{n\,n-1}(V)+C_{n-1\,n}(V)+C_{n\,n}(H_0)+C_{n\,n}(V)\ . \tag{8}$$

In Eq. (8), $C_{nn'}(A)$ is defined by

$$C_{nn'}(A)=\sum_{l_1}\cdots\sum_{l_n}\sum_{l'_1}\cdots\sum_{l'_{n'}}\prod_{m=1}^{n}\left\langle 0\left|\frac{i}{\hbar}\int_0^\infty dt\,e^{-0^+t}e^{iH_0t/\hbar}\tilde{V}e^{-iH_0t/\hbar}\right|l_m\right\rangle$$
$$\times\prod_{m'=1}^{n'}\left\langle l'_{m'}\left|\frac{-i}{\hbar}\int_{-\infty}^{0}dt\,e^{0^+t}e^{iH_0t/\hbar}\tilde{V}e^{-iH_0t/\hbar}\right|0\right\rangle$$
$$\times\frac{\langle l_1,\ldots,l_n\,|\,A\,|\,l'_1,\ldots,l'_{n'}\rangle_c}{n!n'!}\ , \tag{9}$$

where the subscript c represents the instruction to take only connected diagrams into account, $|\,l\rangle$ denotes a ($2e$-$2h$) state in which two electrons below the Fermi surface are excited above it and leave two holes, and $|\,l_1,\ldots,l_n\rangle$ is a state composed of n such ($2e$-$2h$) states which are uncorrelated to each other.

B. Correlation energy

In the two-body approximation, we neglect $E^{(n)}$ for $n\geqq 2$. Thus the correlation energy ε_c is given by $E^{(1)}/N$. In Fig. 1, we represent terms in $E^{(1)}$ by Goldstone diagrams. [Since the contribution of $C_{10}(V)$ is the same as that of $C_{01}(V)$, the diagrams for $C_{10}(V)$ are not drawn in the figure.] Once a diagram is given, we can obtain an expression for the term easily. For example, $C_{01}^{(e)}(V)$ is given by

$$C_{01}^{(e)}(V)=\tfrac{1}{2}\sum_{\mathbf{q},\mathbf{k},\mathbf{k}'}\sum_{\sigma}V(q)\tilde{V}(\,|\,\mathbf{k}'-\mathbf{k}-\mathbf{q}\,|\,)\frac{n_{\mathbf{k}\sigma}(1-n_{\mathbf{k}+\mathbf{q}\sigma})n_{\mathbf{k}'\sigma}(1-n_{\mathbf{k}'-\mathbf{q}\sigma})}{\varepsilon_{\mathbf{k}+\mathbf{q}}-\varepsilon_{\mathbf{k}}+\varepsilon_{\mathbf{k}'-\mathbf{q}}-\varepsilon_{\mathbf{k}'}} \tag{10}$$

$$=\tfrac{1}{2}\sum_{\mathbf{q},\mathbf{k},\mathbf{k}'}\sum_{\sigma}V(q)\tilde{V}(\,|\,\mathbf{k}'+\mathbf{k}+\mathbf{q}\,|\,)\frac{n_{\mathbf{k}\sigma}(1-n_{\mathbf{k}+\mathbf{q}\sigma})n_{\mathbf{k}'\sigma}(1-n_{\mathbf{k}'+\mathbf{q}\sigma})}{\varepsilon_{\mathbf{k}+\mathbf{q}}-\varepsilon_{\mathbf{k}}+\varepsilon_{\mathbf{k}'+\mathbf{q}}-\varepsilon_{\mathbf{k}'}}\ , \tag{10'}$$

with the Fermi distribution function $n_{\mathbf{k}\sigma}$ at $T=0$. Equation (10′) is obtained from Eq. (10) with the use of the fact that $\varepsilon_{\mathbf{k}}=\varepsilon_{-\mathbf{k}}$ and $\tilde{V}(\,|\,\mathbf{q}\,|\,)=\tilde{V}(\,|\,-\mathbf{q}\,|\,)$. Refer to Sec. II B of I for other terms.

Although there are twelve terms in $C_{11}(V)$, they can be grouped into three: the ring family [$C_{11}^{(1d)}(V)$, $C_{11}^{(1e)}(V)$, $C_{11}^{(2d)}(V)$, and $C_{11}^{(2e)}(V)$], the self-energy family [$C_{11}^{(3d)}(V)$ and $C_{11}^{(3e)}(V)$], and the ladder family [$C_{11}^{(4d)}(V)$, $C_{11}^{(4e)}(V)$, $C_{11}^{(5d)}(V)$, $C_{11}^{(5e)}(V)$, $C_{11}^{(6d)}(V)$, and $C_{11}^{(6e)}(V)$]. For the processes of small momentum transfer q, the ring family gives the most important contribution, while for those of large q, the ladder family, in particular, $C_{11}^{(4d)}(V)$ and $C_{11}^{(4e)}(V)$, dominate others.

C. Numerical procedure

We evaluate each term in $E^{(1)}$ numerically in much the same way as in I. We first make a table of a "weight function" for each term in $E^{(1)}$. For example, $C_{01}^{(e)}(V)$ is rewritten as

$$C_{01}^{(e)}(V)=N\int_0^\infty dq\,q^2\phi(q)\int_0^\infty dq'q'^2\tilde{\phi}(q')w_1(q,q')\ , \tag{11}$$

with $\phi(q)\equiv V(q)/(4\pi e^2/k_F^2)$ and $\tilde{\phi}(q')\equiv\tilde{V}(q')/(4\pi e^2/k_F^2)$. We can obtain the weight function $w_1(q,q')$ by performing a four-dimensional integral. Since a two-dimensional integral has to be done afterwards in Eq. (11), we have to make a six-dimensional integral in all to obtain $C_{01}^{(e)}(V)$. In order to check the accuracy of our calculation, we set $\phi(q')$ for $\tilde{\phi}(q')$ in Eq. (11). Then $C_{01}^{(e)}(V)/N$ has been evaluated analytically to be 0.048358.[5] In our numerical calculation, it is found to be 0.048360. Thus for $C_{01}^{(e)}(V)$, we can expect an accuracy of better than 10^{-4}. For terms in $C_{11}(V)$, however, we cannot expect accuracy of the same order, because in general, a six-dimensional integral is necessary for the calculation of weight functions and a nine-dimensional integral is necessary for evaluating $C_{11}(V)$. In fact, the ring family can be calculated rather easily, but it is not an easy task to obtain accuracy of better than 0.1% for terms in the ladder family.

The optimum effective potential can be determined by the functional derivative of $E^{(1)}$:

$$\delta E^{(1)}/\delta\tilde{V}(q)=0\ . \tag{12}$$

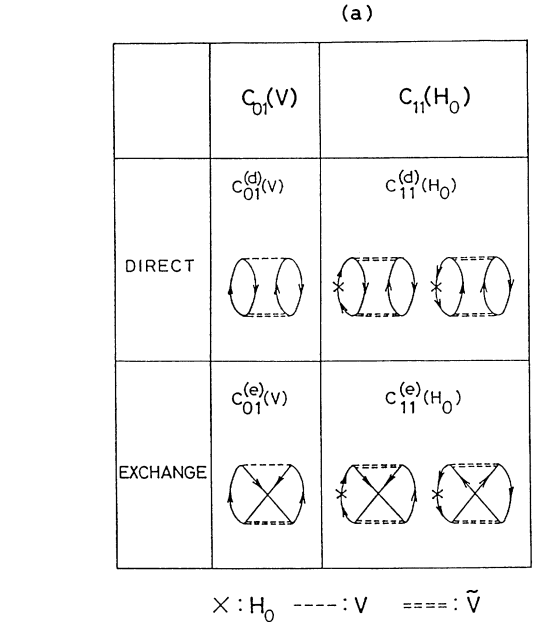

FIG. 1. Goldstone diagrams for $C_{01}(V)$ and $C_{11}(H_0)$ given in (a) and those for $C_{11}(V)$ in (b).

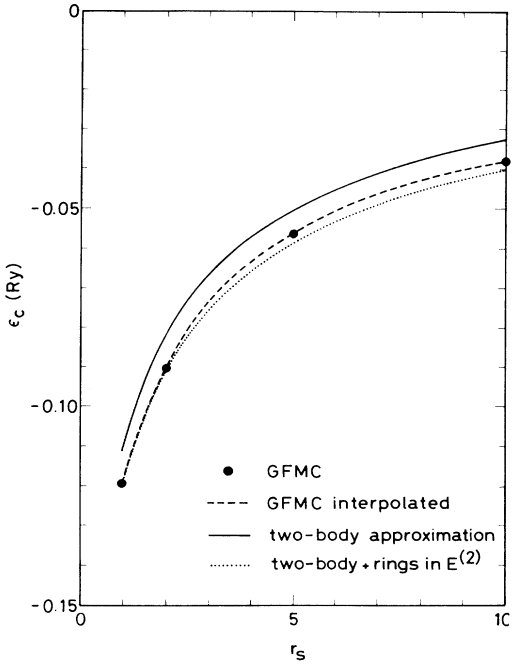

FIG. 2. Correlation energy per electron in units of Ry in the two-body approximation as a function of r_s. The results of the GFMC calculation are also shown by solid points. A dashed curve indicates the results which have been given by the interpolation of those GFMC points. The dotted curve shows the results with addition of terms $C_{12}^{(1d)}(V)$, $C_{22}^{(1d)}(V)$, and $C_{22}^{(d)}(H_0)$ to $E^{(1)}$.

This gives a linear integral equation for $\tilde{V}(q)$. We have solved Eq. (12) by an iterative method. [The iteration is continued until a relative error between old and new $\tilde{V}(q)$'s at each point becomes smaller than 10^{-6}.] For $r_s \leqq 30$, it takes about twenty steps to get a result of $\tilde{V}(q)$. However, for $r_s \geqq 40$, we cannot obtain a convergent result for $\tilde{V}(q)$. We do not think that this arises from some physical reason. We need to obtain terms in $C_{11}(V)$ with better accuracy to get a convergent result for such low-density cases.

D. Results for correlation energy

In Fig. 2, we have shown the calculated results of the correlation energy $\varepsilon_c \equiv E^{(1)}/N$ by a solid curve as a function of r_s. For comparison, the results obtained by the Green's function Monte Carlo (GFMC) method[4] and those by the interpolation through the points of the GFMC calculation[6] are also given by the solid points and dashed curve, respectively. (The results indicated by the dotted curve will be explained in Sec. III.) We have plotted the optimum $\tilde{V}(q)$ in Fig. 3 where instead of $\tilde{V}(q)$, $r_s\tilde{V}(q)$ is shown because this is the expansion parameter of the series (6). There are two remarkable facts in this figure. One is that even if r_s increased by 20 times, the change of $r_s\tilde{V}(q)$ is quite moderate. This is related to the fact that relative errors between our ε_c and those of the GFMC calculation change only slightly with the increase of r_s: They are 7.5%, 9.6%, 11.3%, and 12.1% for $r_s=1$, 5, 10, and 20, respectively. The other is that when $r_s > 9$, $\tilde{V}(q)$ becomes negative for large q. In order to see what terms in $C_{11}(V)$ play an important role in the occurrence of the negative $\tilde{V}(q)$, we have solved Eq. (12) at $r_s=20$ while omitting some terms in $C_{11}(V)$. For example, the dashed curve in Fig. 4 corresponds to the case in which only the electron-electron ladder terms [i.e., $C_{11}^{(4d)}(V)$ and $C_{11}^{(4e)}(V)$] are included in the ladder family, while all other terms in the ring and the self-energy families are taken into account. Although there is a structure at $q=2k_F$, $\tilde{V}(q)$ is always positive in this case. This structure might be related to the problem of a peak in the local-field correction, conventionally denoted by $G(q)$, at $q=2k_F$.[7] (When only the ring term $C_{11}^{(1d)}(V)$ and the electron-electron ladder terms are considered, there is no structure at $q=2k_F$, as shown by a dotted curve in Fig. 4.) On the other hand, the dotted-dashed curve gives the results for

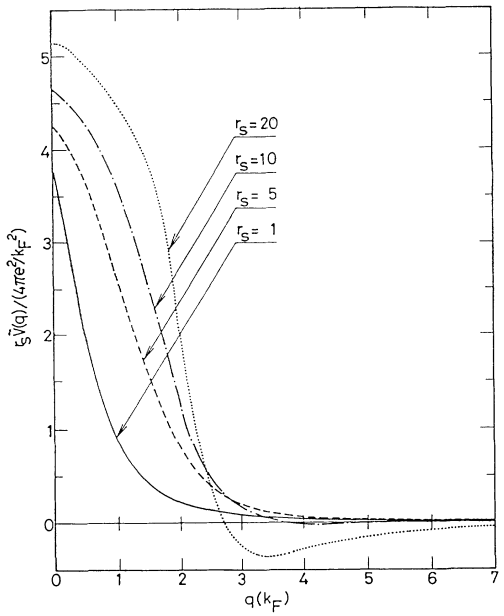

FIG. 3. Effective potential $\tilde{V}(q)$ determined variationally in the two-body approximation through Eq. (12).

the case in which the ring term $C_{11}^{(1d)}(V)$ and all the terms in the ladder family are included. For large q, $\tilde{V}(q)$ becomes negative and is very close to the full calculation which is shown by the solid curve. Thus the negative $\tilde{V}(q)$ is entirely due to the ladder family. In particular, the electron-hole ladder term $C_{11}^{(6d)}$ has a negative sign and

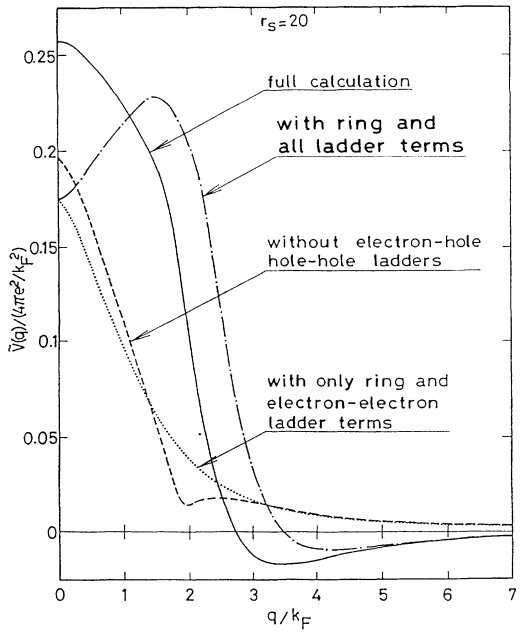

FIG. 4. Effective potential $\tilde{V}(q)$ calculated with omission of various terms in $C_{11}(V)$ at $r_s=20$.

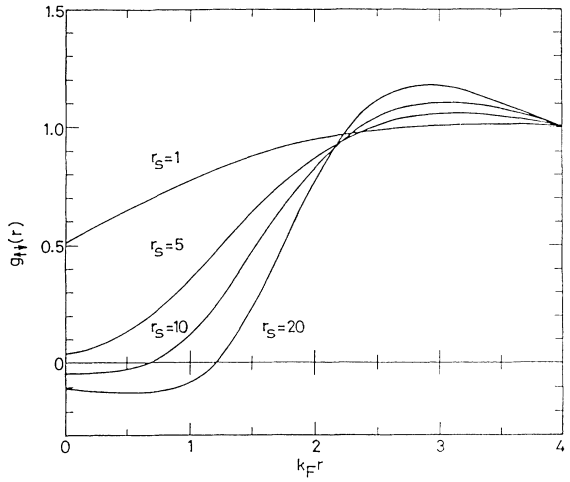

FIG. 5. Spin-antiparallel pair distribution function $g_{\uparrow\downarrow}(r)$ in the two-body approximation for $r_s=1$, 5, 10, and 20.

is found to play a crucial role. It should also be noted that the structure at $q=2k_F$ seen in the dashed curve is washed out in the full calculation.

E. Spin-antiparallel pair distribution function

The spin-antiparallel pair distribution function $g_{\uparrow\downarrow}(r)$ is defined by

$$g_{\uparrow\downarrow}(r)=1+\frac{2}{N}\sum_{\mathbf{q}(\neq 0)} e^{i\mathbf{q}\cdot\mathbf{r}} S_{\uparrow\downarrow}(q) , \tag{13}$$

where the spin-dependent static structure factor $S_{\sigma\sigma'}(q)$ is given by

$$S_{\sigma\sigma'}(q)=\frac{2}{N}\sum_{\mathbf{k},\mathbf{k}'} \langle C_{\mathbf{k}\sigma}^{\dagger} C_{\mathbf{k}+\mathbf{q}\sigma} C_{\mathbf{k}'\sigma'}^{\dagger} C_{\mathbf{k}'-\mathbf{q}\sigma'} \rangle . \tag{14}$$

Thus $g_{\uparrow\downarrow}(r)$ can be expanded in just the same way as $\langle V \rangle$. In the two-body approximation, $g_{\uparrow\downarrow}(r)$ is given by seven terms. The zeroth-order term is just 1 and the first-order one is described diagrammatically by $C_{01}^{(d)}(V)$ with the substitution of $e^{i\mathbf{q}\cdot\mathbf{r}}$ in place of $V(q)/2$. The second-order contribution is composed of terms described diagrammatically by $C_{11}^{(1d)}$, $C_{11}^{(2d)}$, $C_{11}^{(4d)}$, $C_{11}^{(5d)}$, and $C_{11}^{(6d)}$. Figure 5 represents the calculated results of $g_{\uparrow\downarrow}(r)$ for several values of r_s. For $r_s>6.5$, $g_{\uparrow\downarrow}(r)$ becomes negative near $r=0$. This manifestly shows a drawback of the present approximation. As for $g_{\uparrow\uparrow}(r)$, we do not have such a problem and $g_{\uparrow\uparrow}(0)=0$, because we have included direct and exchange terms on the same footing.

III. INCLUSION OF HIGHER-ORDER TERMS

A. Ring family in third and fourth orders

We can improve on the two-body approximation by considering terms in $E^{(2)}$ which is defined in Eqs. (6) and (8). At the present level of computer technology, however, it is probably hopeless that all terms in $E^{(2)}$ can be evaluated accurately enough to obtain a convergent result

of $\tilde{V}(q)$. Thus we must select important terms in $E^{(2)}$. For this purpose, Fig. 3 for $\tilde{V}(q)$ in the two-body approximation is very useful. It suggests that a large correction may come only from small-q processes, because the expansion parameter $r_s\tilde{V}(q)$ has already become so small for q larger than $2k_F$, that higher-order corrections for large-q processes will be negligible. This can also be explained from a physical point of view as follows. For small spatial separations (i.e., large-q case), the four-electron processes which are treated explicitly in $E^{(2)}$ are dominated by the two-electron processes which have already been included in $E^{(1)}$. Thus we need not consider the large-q processes in $E^{(2)}$.

The dominant contribution for small-q processes will come from the ring terms, $C_{12}^{(1d)}(V)$, $C_{22}^{(1d)}(V)$, and $C_{22}^{(d)}(H_0)$, as shown diagrammatically in Figs. 6(a), 6(b), and 6(c). When only these ring terms are added to $E^{(1)}$, we have obtained much better results for ε_c as plotted by a dotted curve in Fig. 2. (The obtained results for $\tilde{V}(q)$ are of course different from those in Sec. II, but convergent results are given for $r_s \leqq 30$, which is just the same as in Sec. II.) However, it is our principle of calculations to consider direct and exchange terms in pairs in order to make $g_{\uparrow\uparrow}(r)$ vanish at $r=0$ when $V(q)/2$ is replaced by $e^{i\mathbf{q}\cdot\mathbf{r}}$. Thus we have to take account of terms like $C_{12}^{(1e)}(V)$ and $C_{22}^{(1e)}(V)$ in addition to the ring terms. We also include the terms $C_{12}^{(2d)}(V)$, $C_{12}^{(3d)}(V)$, $C_{22}^{(2d)}(V)$, and $C_{22}^{(3d)}(V)$ so as to consider the first correction to the ring terms in the calculation of $g_{\uparrow\downarrow}(r)$. The exchange partners of these terms, $C_{12}^{(2e)}(V)$, $C_{12}^{(3e)}(V)$, $C_{22}^{(2e)}(V)$, and $C_{22}^{(3e)}(V)$ are included correspondingly. Other terms in the ring family, such as $C_{12}^{(4d)}(V)$ and $C_{12}^{(5d)}(V)$ in Fig. 6(a) are not considered. This is because the contribution of the sum of $C_{12}^{(4d)}(V)$ and $C_{12}^{(4e)}(V)$ is much smaller than that of the sum of $C_{12}^{(1d)}(V)$ and $C_{12}^{(1e)}(V)$, even though $C_{12}^{(4d)}(V)$ may give a comparable contribution to $C_{12}^{(3e)}(V)$.

Selection of exchange terms in $C_{22}(H_0)$ is made in accordance with that in $C_{12}(V)$. All the singly exchanged terms, i.e., the terms which are obtained by exchanging two pairs of electron-hole lines in the ring diagrams, are shown diagrammatically in $C_{22}^{(e)}(H_0)$ in Fig. 6(c). Each term gives the same contribution and corresponds to the term $C_{12}^{(1e)}(V)$ [or equally $C_{12}^{(2d)}(V)$ or even $C_{12}^{(3d)}(V)$] with the substitution of $-\tilde{V}$ for V. Thus they will be included in our calculations. Selection in the doubly exchanged terms given in $C_{22}^{(ee)}(H_0)$ is much involved. The terms (1) correspond to $C_{12}^{(2e)}(V)$ with the change of V into $-\tilde{V}$ and will be taken into account. The terms (4) correspond to

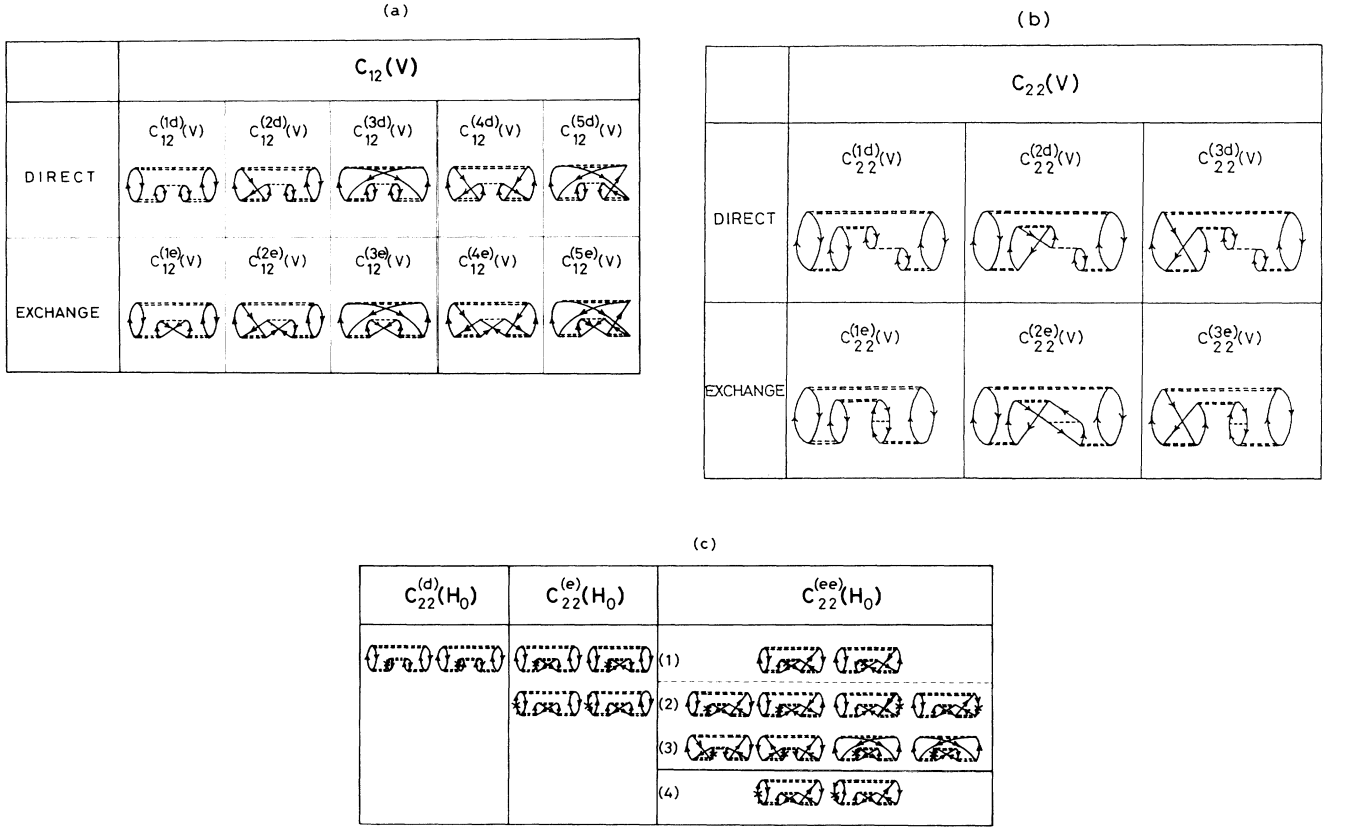

FIG. 6. Goldstone diagrams considered in $E^{(2)}$. Terms in $C_{12}(V)$, $C_{22}(V)$, and $C_{22}(H_0)$ are given in (a), (b), and (c), respectively. Terms, given by $C_{12}^{(4d)}(V)$, $C_{12}^{(4e)}(V)$, $C_{12}^{(5d)}(V)$, and $C_{12}^{(5e)}(V)$, and the terms (4) in $C_{22}^{(ee)}(H_0)$ are not included in the calculation. Half of contributions of the terms (2) and (3) in $C_{22}^{(ee)}(H_0)$ are not considered, either.

$C_{12}^{(5d)}(V)$ and will be neglected. Terms in (2) and (3) produce contributions corresponding to the sum of $C_{12}^{(2e)}(V)$ and $C_{12}^{(5d)}(V)$ and that of $C_{12}^{(3e)}(V)$ and $C_{12}^{(4d)}(V)$, respectively. Thus only a half of contributions should be taken into account for the terms (2) and (3).

Summarizing the selection of terms in $E^{(2)}$, we can write $E^{(2)}$ as

$$E^{(2)}=2C_{12}(V)+C_{22}(V)+C_{22}(H_0)\ , \tag{15}$$

where

$$\begin{aligned}C_{12}(V)&=C_{12}^{(1d)}(V)+C_{12}^{(1e)}(V)+C_{12}^{(2d)}(V)+C_{12}^{(2e)}(V)+C_{12}^{(3d)}(V)+C_{12}^{(3e)}(V)\\&=\tfrac{1}{2}\sum_{\mathbf{q}}\sum_{\mathbf{k}_1\sigma_1}\sum_{\mathbf{k}_2\sigma_2}\sum_{\mathbf{k}_3\sigma_3}\sum_{\mathbf{k}_4\sigma_4}\prod_{i=1}^{4}n_{\mathbf{k}_i\sigma_i}(1-n_{\mathbf{k}_i+\mathbf{q}\sigma_i})\\&\quad\times[(\varepsilon_{\mathbf{k}_1+\mathbf{q}}-\varepsilon_{\mathbf{k}_1}+\varepsilon_{\mathbf{k}_2+\mathbf{q}}-\varepsilon_{\mathbf{k}_2})(\varepsilon_{\mathbf{k}_2+\mathbf{q}}-\varepsilon_{\mathbf{k}_2}+\varepsilon_{\mathbf{k}_3+\mathbf{q}}-\varepsilon_{\mathbf{k}_3})(\varepsilon_{\mathbf{k}_3+\mathbf{q}}-\varepsilon_{\mathbf{k}_3}+\varepsilon_{\mathbf{k}_4+\mathbf{q}}-\varepsilon_{\mathbf{k}_4})]^{-1}\\&\quad\times[-V(q)\tilde{V}(q)^3+\delta_{\sigma_1\sigma_4}V(|\mathbf{k}_1+\mathbf{k}_4+\mathbf{q}|)\tilde{V}(q)^3\\&\qquad+2\delta_{\sigma_1\sigma_2}V(q)\tilde{V}(q)^2\tilde{V}(|\mathbf{k}_1+\mathbf{k}_2+\mathbf{q}|)\\&\qquad-2\delta_{\sigma_1\sigma_2}\delta_{\sigma_1\sigma_4}V(|\mathbf{k}_1+\mathbf{k}_4+\mathbf{q}|)\tilde{V}(q)^2\tilde{V}(|\mathbf{k}_1+\mathbf{k}_2+\mathbf{q}|)\\&\qquad+\delta_{\sigma_2\sigma_3}V(q)\tilde{V}(q)^2\tilde{V}(|\mathbf{k}_2+\mathbf{k}_3+\mathbf{q}|)\\&\qquad-\delta_{\sigma_1\sigma_4}\delta_{\sigma_2\sigma_3}V(|\mathbf{k}_1+\mathbf{k}_4+\mathbf{q}|)\tilde{V}(q)^2\tilde{V}(|\mathbf{k}_2+\mathbf{k}_3+\mathbf{q}|)]\ ,\end{aligned} \tag{16}$$

$$\begin{aligned}C_{22}(V)&=C_{22}^{(1d)}(V)+C_{22}^{(1e)}(V)+C_{22}^{(2d)}(V)+C_{22}^{(2e)}(V)+C_{22}^{(3d)}(V)+C_{22}^{(3e)}(V)\\&=\sum_{\mathbf{q}}\sum_{\mathbf{k}_1\sigma_1}\sum_{\mathbf{k}_2\sigma_2}\sum_{\mathbf{k}_3\sigma_3}\sum_{\mathbf{k}_4\sigma_4}\sum_{\mathbf{k}_5\sigma_5}\prod_{i=1}^{5}n_{\mathbf{k}_i\sigma_i}(1-n_{\mathbf{k}_i+\mathbf{q}\sigma_i})\\&\quad\times[(\varepsilon_{\mathbf{k}_1+\mathbf{q}}-\varepsilon_{\mathbf{k}_1}+\varepsilon_{\mathbf{k}_2+\mathbf{q}}-\varepsilon_{\mathbf{k}_2})(\varepsilon_{\mathbf{k}_2+\mathbf{q}}-\varepsilon_{\mathbf{k}_2}+\varepsilon_{\mathbf{k}_3+\mathbf{q}}-\varepsilon_{\mathbf{k}_3})(\varepsilon_{\mathbf{k}_3+\mathbf{q}}-\varepsilon_{\mathbf{k}_3}+\varepsilon_{\mathbf{k}_4+\mathbf{q}}-\varepsilon_{\mathbf{k}_4})\\&\qquad\times(\varepsilon_{\mathbf{k}_4+\mathbf{q}}-\varepsilon_{\mathbf{k}_4}+\varepsilon_{\mathbf{k}_5+\mathbf{q}}-\varepsilon_{\mathbf{k}_5})]^{-1}\\&\quad\times[V(q)\tilde{V}(q)^4-\delta_{\sigma_1\sigma_5}V(|\mathbf{k}_1-\mathbf{k}_5|)\tilde{V}(q)^4-2\delta_{\sigma_1\sigma_2}V(q)\tilde{V}(q)^3\tilde{V}(|\mathbf{k}_1+\mathbf{k}_2+\mathbf{q}|)\\&\qquad+2\delta_{\sigma_1\sigma_2}\delta_{\sigma_1\sigma_5}V(|\mathbf{k}_1-\mathbf{k}_5|)\tilde{V}(q)^3\tilde{V}(|\mathbf{k}_1+\mathbf{k}_2+\mathbf{q}|)\\&\qquad-2\delta_{\sigma_2\sigma_3}V(q)\tilde{V}(q)^3\tilde{V}(|\mathbf{k}_2+\mathbf{k}_3+\mathbf{q}|)\\&\qquad+2\delta_{\sigma_1\sigma_5}\delta_{\sigma_2\sigma_3}V(|\mathbf{k}_1-\mathbf{k}_5|)\tilde{V}(q)^3\tilde{V}(|\mathbf{k}_2+\mathbf{k}_3+\mathbf{q}|)]\ ,\end{aligned} \tag{17}$$

and $C_{22}(H_0)$ is given by $-C_{12}(\tilde{V})$. In writing Eqs. (16) and (17), we have changed the signs of some momentum variables, as we did in Eq. (10) to obtain Eq. (10′).

B. Numerical procedure

Each term in Eqs. (16) and (17) can be evaluated by the introduction of weight functions as explained in Sec. II C. The effective potential is determined by the equation

$$\frac{\delta(E^{(1)}+E^{(2)})}{\delta\tilde{V}(q)}=0\ . \tag{18}$$

The obtained results for $\tilde{V}(q)$ are, in general, different from those obtained in the preceding section. Quite generally, as we increase the number of terms considered in the series (6), $\tilde{V}(q)$ approaches the bare potential $V(q)$.[1] An example of calculated $\tilde{V}(q)$ is shown in Fig. 7 for the case of $r_s=5$. The solid curve represents the result of the solution of Eq. (18), while the dashed curve corresponds to that of the solution of Eq. (12). (For comparison, the bare potential is shown by a dotted curve.) For q smaller than k_F, the present $\tilde{V}(q)$ becomes larger than the previous one by about 15% [and goes a little bit closer to $V(q)$], but for larger q, they are essentially the same.

For $r_s\leq 10$, we have obtained results for $\tilde{V}(q)$ numerically with no more difficulty than those in the two-body approximation. However, for $r_s>15$, we encounter the same problem as we did at $r_s=40$ in the two-body approximation. Namely, we cannot get a convergent result for $\tilde{V}(q)$. If we remember that a convergent result was obtained even at $r_s=30$ when only the ring terms in $E^{(2)}$ were considered, we can conclude that the less accurate evaluation of exchange terms in $E^{(2)}$ has made the difficulty occur at a much lower value of r_s.

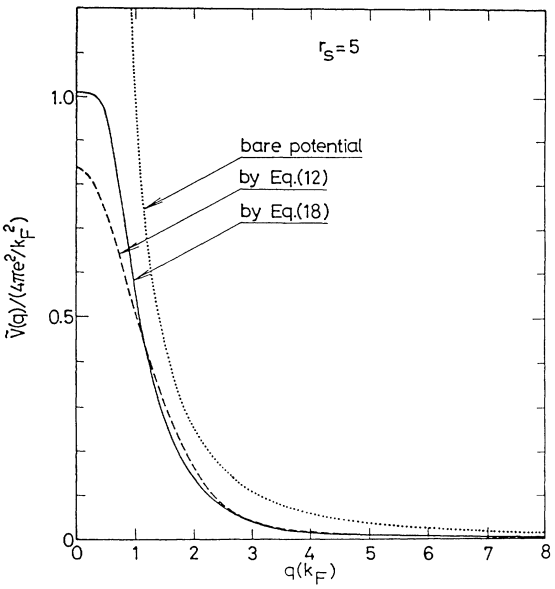

FIG. 7. Effective potential $\tilde{V}(q)$ determined by the solution of Eq. (18), together with that given by Eq. (12). They are, respectively, shown by the solid and dashed curves. Calculations are done at $r_s=5$.

C. Numerical results

The calculated results for the correlation energy are given in units of Ry in the column indicated by $E^{(1)}+E^{(2)}$ in Table I. For comparison, we have also shown the results in the two-body approximation (in the column of $E^{(1)}$), those in the GFMC method,[4,6] those in the coupled-cluster formalism,[8,9] those in the Fermi hypernetted-chain method,[10,11] those in the equation-of-motion approach calculated by Ichimaru and Utsumi,[12] and those in the Green's function method by Suehiro, Ousaka, and Yasuhara (SOY).[13] It is seen that our results are always very close to the GFMC data. The difference is less than 1% and in particular, for $4\leq r_s\leq 8$, our results coincide with them. The accuracy of the present calculation is about the same as that in the coupled-cluster method of Emrich and Zabolitzky.[9] All other previous calculations are less accurate than ours.

To calculate $g_{\uparrow\downarrow}(r)$ in the present calculation, we have to include the terms represented by $C_{12}^{(1d)}$, $C_{12}^{(2d)}$, $C_{12}^{(3d)}$, $C_{22}^{(1d)}$, $C_{22}^{(2d)}$, and $C_{22}^{(3d)}$ in Fig. 6 in addition to the terms already considered in Sec. II E. Figure 8 shows the results of $g_{\uparrow\downarrow}(r)$ for several values of r_s. In contrast with the case in the two-body approximation (Fig. 5), $g_{\uparrow\downarrow}(r)$ is always positive as long as we have obtained a convergent result for $\tilde{V}(q)$. The values of $g_{\uparrow\downarrow}(0)$ are compared with those in the previous calculations in Fig. 9. The solid curve represents the present results. (The dotted one shows those in the two-body approximation.) Results in the Fermi hypernetted-chain approximation are given by the dotted-dashed and double-dotted–dashed curves. They were, respectively, calculated by Lantto[10] and Zabolitzky.[11] The dashed curve shows the results obtained by Yasuhara,[14] who considered only the electron-electron ladder term ($C_{11}^{(4d)}$ term in our notation) and gave an expression for $g_{\uparrow\downarrow}(0)$ as

$$g_{\uparrow\downarrow}(0)=\{2(\alpha r_s/\pi)^{1/2}/I_1[4(\alpha r_s/\pi)^{1/2}]\}^2 , \tag{19}$$

where $I_1(x)$ is the first-order modified Bessel function of the first kind. Although our results agree surprisingly well with those of Yasuhara, there are no reasons why they should coincide with each other. We have considered much more terms like the electron-hole and hole-hole ladders than Yasuhara.

The spin-dependent static structure factors are also calculated and compared with the results very recently given by SOY. In Fig. 10, $S_{\uparrow\downarrow}(q)$ and $S_{\uparrow\uparrow}(q)-S_{\uparrow\uparrow}^{(0)}(q)$ calculated at $r_s=4$ are shown by solid curves, where $S_{\uparrow\uparrow}^{(0)}(q)$ is the static structure factor in the Hartree-Fock approximation, given by

$$S_{\uparrow\uparrow}^{(0)}(q)=\begin{cases}\frac{3}{4}\frac{q}{k_F}-\frac{1}{16}(q/k_F)^3 & \text{for } q<2k_F ,\\ 1 & \text{for } q>2k_F .\end{cases} \tag{20}$$

TABLE I. Correlation energy in Ry units. The first column shows our present results, while the second corresponds to our results in the two-body approximation. The column indicated by GFMC gives the results in the Green's Function Monte Carlo method, obtained from Ref. 4. (Numbers in parentheses are from Ref. 6.) The columns indicated by CC(BL) and CC(EZ) show the results in the coupled-cluster formalism, obtained by Bishop and Lührmann (Ref. 8) and Emrich and Zabolitzky (Ref. 9), respectively. The columns FHNC(L) and FHNC(Z) give the results in the Fermi hypernetted-chain approximation, calculated by Lantto (Ref. 10) and Zabolitzky (Ref. 11), respectively. The column, indicated by IU, shows the results of Ichimaru and Utsumi (Ref. 12). The last column SOY gives the results of Suehiro, Ousaka, and Yasuhara (Ref 13).

r_s	$E^{(1)}+E^{(2)}$	$E^{(1)}$	GFMC	CC(BL)	CC(EZ)	FHNC(L)	FHNC(Z)	IU	SOY
1	−0.119	−0.111	−0.119 (−0.120)	−0.125	−0.122	−0.118	−0.114	−0.1174	−0.1211
2	−0.0891	−0.0821	−0.0902 (−0.0896)	−0.0919	−0.0904	−0.0865	−0.0859	−0.0869	−0.0912
3	−0.0737	−0.0671	(−0.0738)	−0.0743	−0.0738	−0.0709	−0.0710	−0.0711	−0.0757
4	−0.0636	−0.0575	(−0.0636)	−0.0625	−0.0634	−0.0610	−0.0612	−0.0610	−0.0658
5	−0.0563	−0.0506	−0.0563 (−0.0563)	−0.0544	−0.0560	−0.0540	−0.0541	−0.0538	−0.0588
6	−0.0507	−0.0455	(−0.0507)		−0.0505			−0.0483	−0.0534
8	−0.0427	−0.0380	(−0.0427)		−0.0425				
10	−0.0370	−0.0329	−0.03722(−0.0371)		−0.0370	−0.0355	−0.0355	−0.0350	

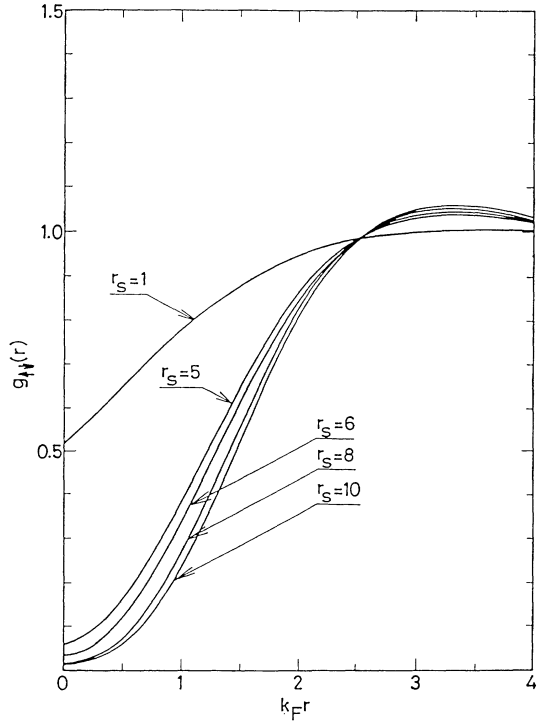

FIG. 8. Spin-antiparallel pair distributions function $g_{\uparrow\downarrow}(r)$ for $r_s=1$, 5, 6, 8, and 10.

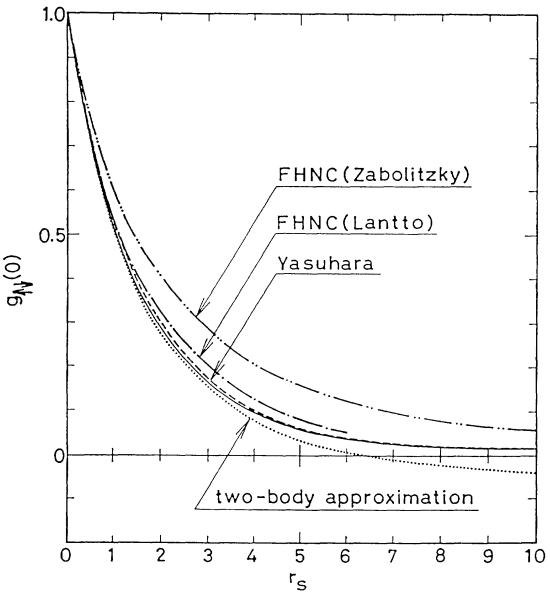

FIG. 9. Values of $g_{\uparrow\downarrow}$ at $r=0$. The solid curve represents the present results, while the dotted shows those in the two-body approximation. The results calculated by Yasuhara (Ref. 13), Zabolitzky (Ref. 11), and Lantto (Ref. 10) are given by the dashed, dotted-dashed, and double-dotted–dashed curves, respectively.

Dashed curves give the results of SOY. The overall feature is the same between the two, but there is a tendency that our $|S_{\sigma\sigma'}(q)|$ becomes smaller for $q \geqq 2k_F$. In Fig. 11, we have given a change of $S_{\uparrow\downarrow}(q)$ as r_s is increased. It is remarkable that at $r_s=10$, $-S_{\uparrow\downarrow}(q)$ has a rather sharp peak near $q=k_F$ and changes its sign near $q=2.5k_F$.

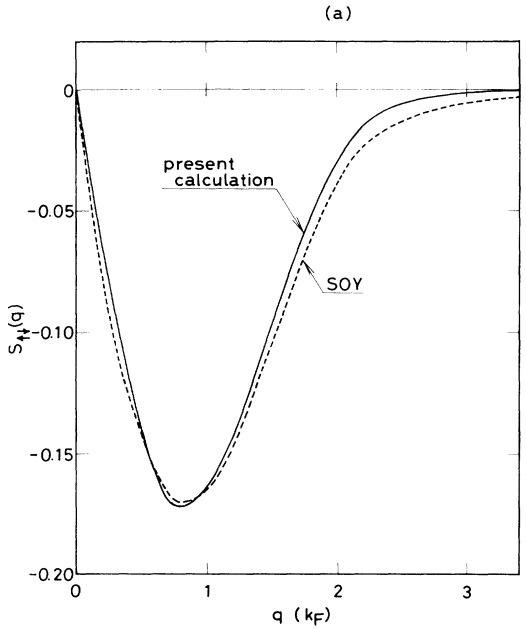

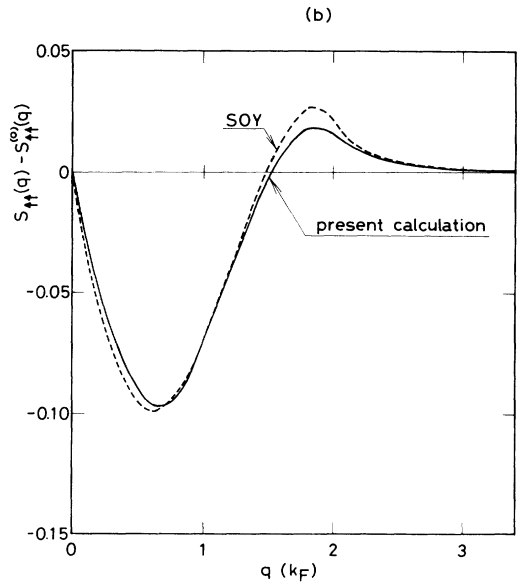

FIG. 10. Spin-dependent static structure factor $S_{\sigma\sigma'}(q)$ calculated at $r_s=4$. In (a) and (b), $S_{\uparrow\downarrow}$ and $S_{\uparrow\uparrow}-S^{(0)}_{\uparrow\uparrow}$ are given by solid curves, respectively, where $S^{(0)}_{\uparrow\uparrow}$ is the static structure factor in the Hartree-Fock approximation. Dashed curves show the results of Suehiro, Ousaka, and Yasuhara (Ref. 13).

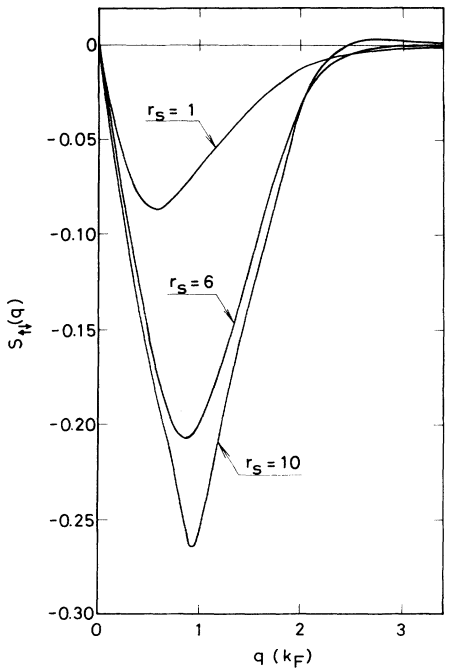

FIG. 11. Dependence of the static structure factor $S_{\uparrow\downarrow}(q)$ on r_s.

IV. CONCLUSION AND DISCUSSION

We have applied successfully the method of effective-potential expansion to an electron gas. Although the two-body approximation only gives the results of the correlation energy with an error of about 10% and also produces the problem of negative $g_{\uparrow\downarrow}(r)$ near $r=0$, we can achieve a great improvement on it by considering some of third- and fourth-order terms in the ring family. The resulting correlation energies in the range of $1 \leqq r_s \leqq 10$ agree quite well with those by the GFMC and the coupled-cluster formalism (the difference is less than 1%).

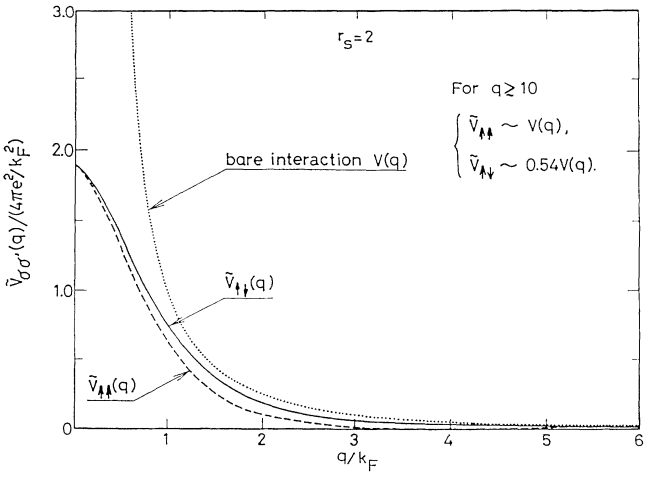

FIG. 12. Spin-dependent effective potential $\tilde{V}_{\sigma\sigma'}(q)$ determined by the solution of Eq. (12') at $r_s=2$.

In general, the effective potential $\tilde{V}$ should depend on spin orientations, as indicated in Eq. (5). The spin dependence of $\tilde{V}$ was discussed in detail in Secs. III C and III E of I for a two-dimensional electron-gas system. The similar argument can also be done for the present case. For example, at $q=0$, $\tilde{V}_{\uparrow\uparrow}$ should be equal to $\tilde{V}_{\uparrow\downarrow}$, but when q is increased slightly, $\tilde{V}_{\uparrow\uparrow}$ should be smaller than $\tilde{V}_{\uparrow\downarrow}$. When q is large enough, $\tilde{V}_{\uparrow\uparrow}$ approached to the bare potential $V(q)$, while $\tilde{V}_{\uparrow\downarrow}$ is much reduced from it. If we replace Eq. (12) by

$$\delta E^{(1)}/\delta \tilde{V}_{\sigma\sigma'}(q)=0 \ , \tag{12'}$$

we can determine $\tilde{V}_{\sigma\sigma'}$ numerically. In Fig. 12, we have shown the results of calculated $\tilde{V}_{\uparrow\uparrow}$ and $\tilde{V}_{\uparrow\downarrow}$ at $r_s=2$. The calculated correlation energy is -0.0821 Ry and is just the same as that with the solution of Eq. (12). Thus for $r_s=2$, it does not matter for the correlation energy whether we consider the spin dependence of $\tilde{V}$ or not. For larger r_s, we cannot get a convergent result for $\tilde{V}_{\sigma\sigma'}$. The problem is that in the equation to determine $\tilde{V}_{\uparrow\uparrow}$, direct and exchange terms enter with the same weight (and the opposite sign). Thus we have to evaluate each term in $E^{(1)}$ with accuracy better than 10^{-4}, but such a level of accuracy is difficult to achieve at present for the calculation of the ladder family. When we include higher-order terms in the calculation of $\langle H \rangle$, it is less important to consider the spin dependence of $\tilde{V}$, because as we include more higher-order terms, $\tilde{V}$ approaches to the bare potential which is evidently independent of spin orientations.

APPENDIX

In this Appendix, we prove rigorously that the cutoff of the cluster expansion (6) at any level always gives an energy larger than the true ground-state energy for sufficiently weak effective potentials. In Sec. II, we have assumed that $\tilde{V}$ is a two-body potential as given in Eq. (5). However, we need not restrict ourselves to that case. Even if we take such a $\tilde{V}$ having an expansion.

$$\tilde{V}=\tilde{V}_2+\tilde{V}_4+\tilde{V}_6+\cdots \ , \tag{A1}$$

where $\tilde{V}_{2n}$ is a $2n$-body interaction part of $\tilde{V}$, we can prove an expansion of Eq. (6) which can be rewritten as

$$\langle H \rangle = \sum_{m=0}^{\infty} \sum_{n=0}^{\infty} \langle 0 \mid L_u(\tilde{U}^{+m}) H L_u(\tilde{U}^{n}) \mid 0 \rangle_c / m!n! \ , \tag{A2}$$

where the operator $\tilde{U}$ is defined by

$$\tilde{U}=-\frac{i}{\hbar}\int_{-\infty}^{0} dt\, e^{0^+ t} \exp(iH_0 t/\hbar)\tilde{V}\exp(-iH_0 t/\hbar) \ . \tag{A3}$$

By defining $\tilde{U}_{2n}$ through Eq. (A3) with the substitution of $\tilde{V}_{2n}$ for $\tilde{V}$, we can rewrite Eq. (A2) further as

$$\langle H\rangle = E^{(0)} + \langle 0 \mid \tilde{U}_2^{+} H \mid 0\rangle_c + \langle 0 \mid H\tilde{U}_2 \mid 0\rangle_c + \langle 0 \mid \tilde{U}_2^{+} H\tilde{U}_2 \mid 0\rangle_c + \tfrac{1}{2}\langle 0 \mid L_u(\tilde{U}_2^{+2})H \mid 0\rangle_c + \langle 0 \mid \tilde{U}_4^{+} H \mid 0\rangle_c + \tfrac{1}{2}\langle 0 \mid HL_u(\tilde{U}_2^{2}) \mid 0\rangle_c + \langle 0 \mid H\tilde{U}_4 \mid 0\rangle_c + \cdots . \tag{A4}$$

Now for a given $\tilde{V}_2$, we can choose $\tilde{V}_{2n}$'s for $n \geqq 2$ so that the higher-order terms in Eq. (A4) vanish order by order. As a result, we have an expression for $\langle H\rangle$ having only first four terms in Eq. (A4).

In fact, by choosing $\tilde{V}_{2n}$ so as to satisfy

$$\tilde{U}_{2n} = \frac{(-1)^{n-1}}{n} L_u(\tilde{U}_2^{n}) , \tag{A5}$$

we obtain

$$\langle H\rangle = E^{(0)} + E^{(1)} , \tag{A6}$$

with $E^{(1)}$ defined by Eqs. (8) and (9) with the substitution of $\tilde{V}_2$ for $\tilde{V}$. Since Eq. (A6) is exact for a trial function having the form of Eq. (4) with $\tilde{V}$ defined by Eqs. (A1), (A3), and (A5), this equation gives a variational upper bound to the true ground-state energy. However, this is true only when $\tilde{V}$ (or equivalently $\tilde{U}$) determined from Eqs. (A1) and (A5) is finite. The radius of the convergence circle in terms of $\tilde{U}_2$ is readily known to be unity from Eq. (A5). Thus for a sufficiently weak effective interaction $\tilde{V}_2$, the upper-bound property holds, but for large $|\tilde{V}_2|$, it is not guaranteed.[15]

When we define $\tilde{U}_{2n}$ by

$$\tilde{U}_{2n} = 2\cos\left[\frac{\pi n}{4}\right]\frac{(-1)^{n-1}}{n} L_u[(\tilde{U}_2/\sqrt{2})^n] , \tag{A7}$$

instead of Eq. (A5), we obtain

$$\langle H\rangle = E^{(0)} + E^{(1)} + E^{(2)} , \tag{A8}$$

with $E^{(n)}$ given by the substitution of $\tilde{V}_2$ for $\tilde{V}$ in Eqs. (8) and (9). Again for small $\tilde{V}_2$, Eq. (A8) is always larger than the true ground-state energy. Compared with Eq. (A5), the radius of the convergent circle becomes $\sqrt{2}$ times as large as before. Thus the upper-bound property holds for a wider class of effective potentials $\tilde{V}_2$ in this case. In a similar way, we can define $\tilde{U}_{2n}$ so that we obtain

$$\langle H\rangle = \sum_{n=0}^{m} E^{(n)} , \tag{A9}$$

for any positive integer m. Note that the case $m = \infty$ is special in the sense that the radius of the convergence circle is infinite to make the upper-bound property hold for any $\tilde{V}_2$.

[1] Y. Takada, Phys. Rev. A **28**, 2417 (1983).

[2] Y. Takada, Phys. Rev. B **30**, 3882 (1984).

[3] D. Ceperley, Phys. Rev. B **18**, 3126 (1978).

[4] D. M. Ceperley and B. J. Alder, Phys. Rev. Lett. **45**, 566 (1980).

[5] L. Onsager, L. Mittag, and M. J. Stephen, Ann. Phys. (N.Y.) **18**, 71 (1986).

[6] S. H. Vosko, L. Wilk, and M. Nusair, Can. J. Phys. **58**, 1200 (1980).

[7] A. W. Overhauser, Phys. Rev. B **2**, 874 (1970); F. Toigo and T. O. Woodruff, *ibid.* **2**, 3958 (1970); **4**, 4312 (1971); P. Vashista and K. S. Singwi, *ibid.* **6**, 875 (1972); A. Holas, P. K. Arvind, and K. S. Singwi, *ibid.* **20**, 4912 (1979); F. Brosen, J. T. Devreese, and L. F. Lemmens, *ibid.* **21**, 1363 (1980); K. Utsumi and S. Ichimaru, Phys. Rev. A **26**, 603 (1982); L. Lantto, P. Pietilainen, and A. Kallio, Phys. Rev. B **26**, 5568 (1982); Y. R. Wang, M. Ashraf, and A. W. Overhauser, *ibid.* **30**, 5580 (1984).

[8] R. F. Bishop and K. H. Lührmann, Phys. Rev. B **26**, 5523 (1982).

[9] K. Emrich and J. G. Zabolitzky, Phys. Rev. B **30**, 2049 (1984).

[10] L. J. Lantto, Phys. Rev. B **22**, 1380 (1980).

[11] J. G. Zabolitzky, Phys. Rev. B **22**, 2353 (1980).

[12] S. Ichimaru and K. Utsumi, Phys. Rev. B **24**, 7385 (1981).

[13] H. Suehiro, Y. Ousaka, and H. Yasuhara, J. Phys. C **19**, 4263 (1986).

[14] H. Yasuhara, Solid State Commun. **11**, 1481 (1972); J. Phys. Soc. Jpn. **36**, 361 (1974).

[15] H. Shiba kindly informed the author that in the one-dimensional Hubbard model at the half-filled band, this upper-bound property is violated in the sufficiently strong on-site Coulomb interaction case.